Analytical Methods

Accepted Manuscript

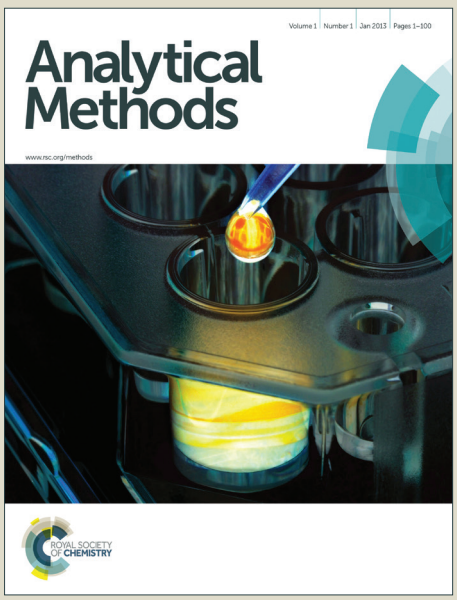

ROYAL SOCIETY OF CHEMISTRY

www.rsc.org/methods

Cite this: DOI: 10.1039/c0xx00000x

www.rsc.org/xxxxxx

ARTICLE TYPE

Colorimetric copper (II) ion sensor based on the conformational change of peptide immobilized onto the surface of gold nanoparticles

Hongxia Chen[a], Jiangjiang Zhang[a], Xinjian Liu[b], Yanmin Gao[a], Zonghuang Ye[b], Genxi Li *[a,b]

Received (in XXX, XXX) Xth XXXXXXXXX 20XX, Accepted Xth XXXXXXXXX 20XX

DOI: 10.1039/b000000x

Detection of heavy metal ions has attracted great attentions, and colorimetric assay has remarkable advantages, such as convenient, efficient, free-equipment and always visible. Herein, we report a highly sensitive and selective colorimetric sensor for the determination of copper (II) ions based on the conformational change of Cu^{2+}-binding peptides immobilized onto the surface of gold nanoparticles. In the presence of copper (II) ions, the peptides modified gold nanoparticles (p-AuNPs) will cooperatively bind together, resulting in aggregation and precipitation of the p-AuNPs, thus color change can be observed from wine red to colorless. Nevertheless, other cations like Mg^{2+}, Ca^{2+}, Zn^{2+}, Fe^{3+}, Pb^{2+}, Mn^{2+}, Ba^{2+}, Ni^{2+}, Co^{2+}, K^{+} and Ag^{+} cannot have such effect, so no obvious disturbance occurs in the same concentration to Cu^{2+}. With this well-designed sensing platform, the detection range of copper (II) ions is found to be 10-150 μM, which falls into the maximum accepted level of 1.3 ppm (~20 μM) as set by the U.S. Environmental Protection Agency. Moreover, modification of AuNPs with differential binding peptides may provide new and simple platforms for the detection of other heavy metal ions, so the strategy proposed for the detection of Cu^{2+} in this work can be extended for more applications in the future.

1. Introduction

Colorimetric sensor based on gold nanoparticles (AuNPs) has been developed to be a powerful platform since the first DNA sensor was reported by Mirkin and co-workers.[1] Due to its remarkable optical properties including high extinction coefficient and adjustable plasmon band,[2-4] this simple and versatile sensing platform has been increasingly applied for the determination of a large variety of targets, such as proteins,[5, 6] nucleic acids,[7, 8] saccharides,[9] small molecules,[10-12] metal ions,[13-15] and living cells[16, 17]. Taking advantage of the color change that arises from the interparticle plasmon coupling during AuNPs aggregation (red-to-purple or blue) or redispersion of AuNPs aggregates (purple-to-red),[18] it is quickly becoming an important alternative to conventional detection techniques (e.g., fluorescence-based assays) and holds great potential in clinical diagnostics, drug discovery and environmental contaminant analysis.[19]

In recent years, great efforts have been committed to the determination of copper (II) ions in the field of environmental and biological systems because of its potential toxicity on human health and ecosystem. Cu^{2+} plays an essential role in physiological processes in certain amounts, including energy generation, dioxygen transport and activation, and signal transduction.[20] However, at elevated concentrations, Cu^{2+} can react with molecular oxygen to generate reactive oxygen species (ROS), suggesting their potential damage to proteins, nucleic acids and lipids.[21, 22] Additionally, the cellular toxicity of Cu^{2+} ion is related to some neurodegenerative diseases such as Menkes and Wilson disease, hereditary aceruloplasminemia, prion disease and Alzheimer's disease.[23-25] In this regard, the residual level of Cu^{2+} in drinking water is restricted. For example, the United States Environment Protection Agency (USEPA) sets a maximum contaminant level (MCL) of Cu^{2+} at 1.3 ppm (~20 μM) in drinking water. Therefore, it is important to develop highly sensitive and selective analytical methods for Cu^{2+} detection.

Numerous spectrofluorimetric and spectrophotometric techniques have been used for the individual determination of Cu^{2+} ion.[26-39] Although a few probes are able to detect Cu^{2+} with high sensitivity, selectivity and fast response, these probes involve relatively complex organic synthesis, high expensive labeling reagents, organic solvents or a narrow detection range, which may hinder their potential applications. Therefore, it still remains imperative to develop simple, cost-efficient, sensitive and selective colorimetric sensors for Cu^{2+} determination.

In this study, a highly selective and sensitive colorimetric assay has been developed for the determination of copper (II) ions by using peptides modified AuNPs (p-AuNPs). The Cu^{2+}-binding peptide Ser-Ile-Arg-Lys-Leu-Glu-Tyr-Glu-Ile-Glu-Glu-Leu-Arg-Leu-Arg-Ile-Gly (SIRKLEYEIEELRLRIG)[40] used here takes α-helical conformation with good hydrophilicity. However, in the presence of Cu^{2+}, interaction between carboxyl residuals of the peptide and Cu^{2+} induces a conformational change from α-helix to β-sheet, which results in decreasing hydrophilicity and aggregations of the peptides. Taking this advantage of Cu^{2+}-binding peptide, we propose the attachment of the Cu^{2+}-binding peptide to the surface of AuNPs, thus, in the presence of copper

(II) ions, selective aggregation of p-AuNPs would be observed (Scheme 1). To achieve this goal, a spacer of four amino acid residues Ac-Cys-Gly-Gly-Gly (Ac-CGGG) is designed to be added to the N-terminal of the Cu^{2+}-binding peptide. While the forming of Au-S bond through sulfhydryl group of Cys residue ensures the covalently binding of the peptide to AuNPs, the spacer avoids perturbation of peptides' conformation when covalently immobilization to the surface of AuNPs. The as-prepared p-AuNPs can show excellent selectivity and sensitivity on sensing copper (II) ions, when contrasted to other metal cations including Mg^{2+}, Ca^{2+}, Zn^{2+}, Fe^{3+}, Pb^{2+}, Mn^{2+}, Ba^{2+}, Ni^{2+}, Co^{2+}, K^{+} and Ag^{+}. This colorimetric Cu^{2+} sensor also avoids the usage of expensive labeling reagents and displays a well detection range of 10~150 μM which falls into the maximum accepted level of 1.3 ppm (~20 μM) as set by USEPA.

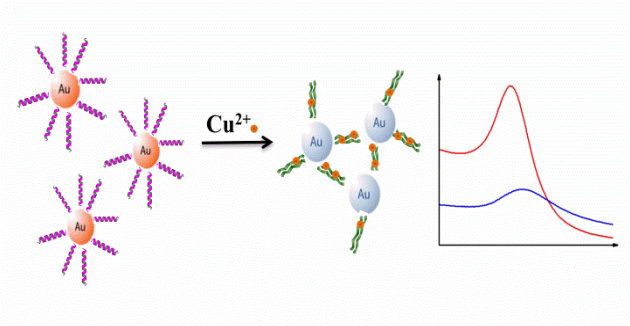

Scheme 1 Illustration of copper (II) ions induced p-AuNPs aggregation

2. Experimental section

2.1 Materials

Gold (III) chloride trihydrate ($HAuCl_4 \cdot 3H_2O$), sodium citrate tribasic dehydrate, Tris(2-carboxyethyl)phosphine hydrochloride (TCEP), N-2-Hydroxyethylpiperazine- N'-2-ethanesulfonic acid (HEPES), dimethyl sulfoxide (DMSO) were obtained from Sigma-Aldrich (St. Louis, MO, USA). Cu^{2+}-binding peptide with a sequence of Ac-CGGGSIRKLEYEIEELRLRIG-NH_2 was synthesized by Sangon Biotch Co. Ltd. (Shanghai, China). Metal salts of $CuCl_2$, $MgCl_2$, $CaCl_2$, $ZnCl_2$, $FeCl_3$, $PbCl_2$, $MnCl_2$, $BaCl_2$, $NiCl_2$, $CoCl_2$, $AgNO_3$ and KCl were purchased from Sigma-Aldrich (St. Louis, MO, USA). Bovine serum albumin (BSA) was supplied by Zhaorui Biotech Co. Ltd. (Shanghai, China). The ultra-pure water (18.2 MΩ·cm) was purified with a Millipore Milli-Q water system.

2.2 Synthesis of AuNPs

AuNPs (2.3 nM) with an approximate diameter of 13-nm was synthesized based on a reported protocol.[41] Briefly, an aqueous solution of $HAuCl_4$ (0.01%, 100 mL) was heated under a vigorous stirring in a 250 ml round-bottom flask fitted with a reflux condenser. Trisodium citrate (1%, 3.5 mL) was one-time rapidly added to the solution after boiling 2-3 minutes. Heating under reflux was continued for an additional 15 min, during which time the color changed from deep-blue to wine-red. The solution was cooled to room temperature with continuous stirring and stored in 4 °C. UV-vis spectra of the as-prepared AuNPs displayed a maximum absorption band at 520 nm.

2.3 Preparation of p-AuNPs

Due to the possible perturbation between the C-terminal free carboxyl and copper (II) ions, the C-terminal of Cu^{2+}-binding peptide is blocked with amine. The secondary structure of the peptide was predicted with α-helix from Ser5 to Glu21 and a random-coil from Cys1 to Glu4 by PSIPRED V3.3 (UCL, UK). This means the added sequence CGGG has no disturbance on the functional conformation. The Cu^{2+}-binding peptide was used without any purification process and dissolved in HEPES buffer solution (10 mM, 10 mM TCEP, 1% DMSO, pH 8.0) with a concentration of 1 mg/mL (~0.4 mM) as stored solution. 20 μL of stored solution was pipetted into 480 μL HEPES (10 mM, 0.15 μM BSA, pH 8.0) and mixed as the modification solution. Before incubation with peptide solution, 0.5 mL AuNPs was centrifuged (4 °C, 12000 rpm, 20 min) and washed with ultra-pure water for two times. The precipitate was resuspended into 0.5 mL modification solution and incubated overnight under 4 °C. The gold nanoparticle/peptide solution was then centrifuged (4 °C, 10000 rpm, 20 min). The resulting sediment was then resuspended in 0.5 mL HEPES (10 mM, pH 8.0).[42-44]

2.4 Apparatus and spectral measurements

A UV-vis spectrophotometer (UV-2450) purchased from Shimadzu Co. (Kyoto, Japan) was used for all absorption measurements. Quartz cuvettes with an optical path length of 10-mm and a volume of 50 μL were used. All measurements were performed at room temperature. A mixture solution of 45 μL p-AuNPs and 5 μL Cu^{2+} with appropriate concentration was pipetted into the cell after incubation for spectra measurement. ζ -potential and hydrophobic diameter were determined with a Zetasizer 3000HS apparatus (Malvern Instruments Ltd., Malvern, UK). And digital images were taken by a Panasonic DMC-LX5 camera

3. Results and discussion

3.1 Characterization of p-AuNPs

The p-AuNPs are prepared by incubating excess Cu^{2+}-binding peptide with AuNPs. The peptide is covalently attached to the surface of AuNP through Au-S bond. The N-terminal Cys which holds the free sulfhydryl group is proposed to bind to the Au atom on the surface of nanoparticles. Replacement of negatively charged citrate to neutrally charged peptide may induce a ζ -potential loss from -29.4 mV to -13.6 mV (Table 1). Figure 1A shows the change in the absorption spectrum of the AuNPs before and after the peptide immobilization. Prior to the modification, the citrate-protected 13-nm AuNPs exhibit a surface plasmon resonance band at 520 nm. Replacing the citrate with peptide, which increases the localized refractive index,[45] produces a red-shift to 525 nm. The 5 nm wavelength shift indicates the binding of peptides to AuNPs. Moreover, the increase of hydrophobic diameter from 14.8 nm to 19.0 nm presented in the dynamic light scattering (DLS) spectra also validates the formation of p-AuNPs (Figure 1B). According to the decrease of UV absorbance of modification solution at 280 nm (ε =1280 M^{-1} cm^{-1})[40], the molecule number of peptide immobilized on surface of AuNPs is 1359 per AuNPs. And the coverage of the surface is estimated of 50.26%.

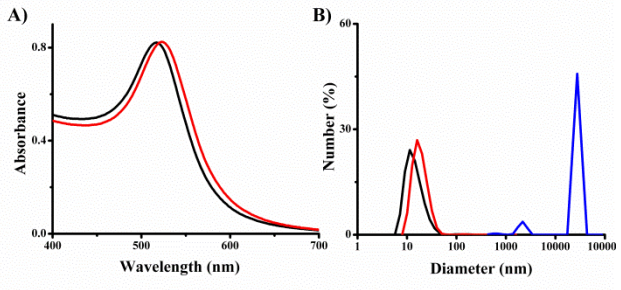

Fig. 1 A) UV-vis absorption spectra of AuNPs before (black trace) and after (red trace) covalently immobilization of the Cu2+-binding peptide, i.e.p-AuNPs. B) DLS spectra of AuNPs (black trace), p-AuNPs (red trace), and the p-AuNPs in the presence of 100 μM Cu^{2+} (blue trace). The data were measured in 10 mM HEPES (pH 8.0) at room temperature.

Table 1 ζ -potential of AuNPs , p-AuNPs, and p-AuNPs attached with Cu^{2+}.

	AuNPs	p-AuNPs	p-AuNPs/Cu^{2+}
ζ -potential (mV)	-29.4	-13.6	0.2

3.2 Cu^{2+} induced aggregation of AuNPs and p-AuNPs

It is reported that plasmon coupling between AuNPs dependents on the interparticle distance.[46, 47] During the aggregation of AuNPs, as particles getting closer, shift in UV-vis absorption spectrum can be observed. The UV-vis maximum absorption peak shifts to the longer wavelength and the color changes from red to purple and then to blue. Figure 2 shows the red-shift of UV-vis absorption peak of AuNPs and p-AuNPs which induced by copper (II) ions. In case of AuNPs, the peak at 520 nm decreases, while a new peak at 642 nm appears in the presence of Cu^{2+}. The color changes from red to blue which means a typical aggregation of AuNPs progressed, while a shift of 122 nm is observed. This aggregation is due to the loss of net charge of negatively charged AuNPs after binding with the positively charged copper (II) ions. However, this aggregation is not selective to Cu^{2+}, because other multivalent cations can also lead to such aggregation. Therefore, bare AuNP cannot be used to sensing Cu^{2+} directly. For p-AuNPs, the maximum absorption peak at 525 nm shifts to 556 nm after selectively binding with Cu^{2+}. The aggregation and precipitation of p-AuNPs can also be observed while the solution is changed from red to colorless. The peak shift in the UV-vis absorption spectrum is also due to the interparticle distance between the p-AuNPs during the aggregations. Cetainly, the unmodified AuNPs can directly bind together without distinct space. However in case of p-AuNPs, the immobilized peptide will prevent further close to the surrounding p-AuNPs during aggregation. Therefore, Cu^{2+} induced red-shift of p-AuNPs is only 31 nm.[48] The only BSA-adsorbed AuNPs shows no obvious change under the same concentration of copper (II) ions (Fig. S1). *Canary et al.* had described the interaction between peptide (SIRELEAKIRELELRIG) and copper (II) ions.[40] These results suggest the interaction between p-AuNPs and Cu^{2+} drives the conformational change. On one hand, the conformational change of peptides decreases its hydrophilicity, which will destabilize the p-AuNPs. On the other hand, Cu^{2+} mediated interaction between peptides immobilized on interparticles directly aggregates the p-AuNPs. Nevertheless, due to the slight red-shift of the absorption peak induced by copper (II) ions, color change can be observed, so it is possible to make use of the color and the absorbance decrease at 520 nm to determinate various concentrations of copper (II) ions.

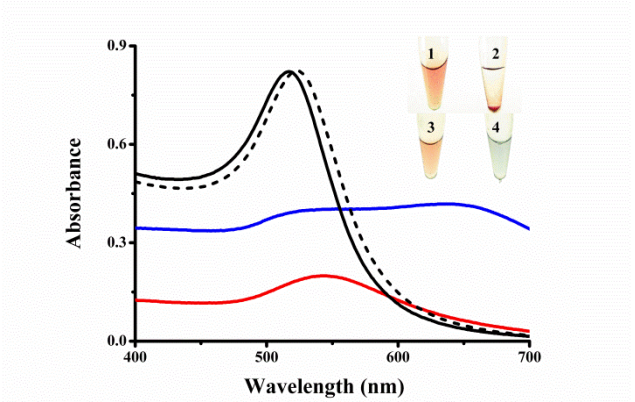

Fig. 2 UV-vis absorption spectra of the proposed sensor for the measurement of copper (II) ions by using p-AuNPs (red trace) and unmodified AuNPs (blue trace). The black solid line represents AuNPs without Cu^{2+}, and the black dash line stands for p-AuNPs without Cu^{2+}. Inset: digital images recorded after incubation with or without copper (II) ions. 1: p-AuNPs (Cu^{2+}/0 μM); 2: p-AuNPs (Cu^{2+}/100 μM); 3: AuNPs (Cu^{2+}/0 μM); 4: AuNPs (Cu^{2+}/100 μM).

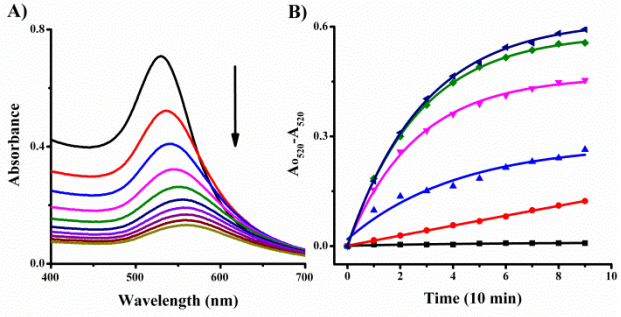

Fig. 3 A) UV-vis absorption spectra of p-AuNPs after the addition of 100 μM Cu^{2+}, the recording time from top to bottom is 0 min, 10 min, 20 min, 30 min, 40 min, 50 min, 60 min, 70 min, 80 min, and 90 min, respectively. B) Calibration curves of time related absorbance change of p-AuNPs at 520 nm under various concentrations of copper (II) ions (from bottom to top, the concentration is 0 μM, 10 μM, 20 μM, 30 μM, 50 μM, 80 μM and 100 μM, respectively).

3.3 Time dependent measurement

As is shown in Figure 3A, after addition of copper (II) ions in the p-AuNPs solution, a progressive aggregation of p-AuNPs with the continuous decrease of UV-vis absorption at 520 nm can be observed. To get well distinguishable UV-vis absorption spectra upon different concentrations of Cu^{2+}, the time related curves

have also been measured with various concentrations of Cu^{2+}, as is shown in Figure 3B. The vertical coordinates Ao_{520}-A_{520} stands for the change of UV absorbance at 520 nm. Ao_{520} represents the initial UV absorbance at 520 nm while A_{520} is time-depended. Without any copper (II) ions existing, there is no obvious change on the absorbance which demonstrates the stability of p-AuNPs. However, in the presence of various concentrations Cu^{2+}, a progressive decrease of absorbance at 520 nm can be detected. Under the low concentration conditions, the absorbance changes are distinguished well upon the incubation times. Meanwhile, at the higher concentrations, it is not well enough to discriminate the UV-vis absorbance changes until the incubation time getting longer to 90 minutes. Therefore, an incubation time of 90 minutes is used for the following measurements.

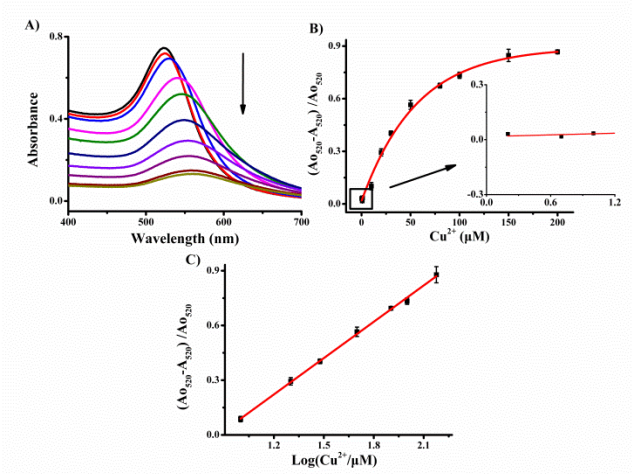

Fig. 4 A) UV-vis absorption spectra of p-AuNPs in the presence of a series concentration of copper (II) ions. From top to ground, concentration of spectra is 0 μM, 1 μM, 10 μM, 20 μM, 30 μM, 50 μM, 80 μM, 100 μM, 150 μM and 200 μM. B) Relationship between the absorbance change and the concentrations of copper (II) ions. The Inset shows an enlarged portion area bounded by the dashed box. C) Linear fitting curve of absorbance change at 520 nm versus logarithm of concentration of Cu^{2+} from 10 μM to 150 μM. The scale bars represent the standard deviations of three replicated samples.

3.4 Concentration dependent measurement

Figure 4A shows the UV-vis absorption spectra of p-AuNPs in the presence of series concentrations of copper (II) ions. With concentration of Cu^{2+} increasing, the absorbance at 520 nm gets lower. And the maximum absorption peak shifts to the longer wavelength. The absorbance change (Ao_{520}-A_{520})/Ao_{520} at 520 nm has been exhibited in Figure 4B, where Ao_{520} represents absorbance at 520 nm without Cu^{2+} while A_{520} involves to the absorbance after incubation with related concentrations of Cu^{2+}. When the concentration of Cu^{2+} is lower than 1 μM, no obvious absorbance change can be observed. As the concentration gets higher, the absorbance at 520 nm decreases, and it reaches an equilibrium point at the concentration of 150 μM. There is no further obvious change observed if a higher concentration of Cu^{2+} is applied. The fitting curve shows an excellent linear detection range from 10 μM to 150 μM with an R^2 of 0.99853 (Figure 4C). And the detection limit was 1μM. It is broader than the detection range of some other sensors (Table 2). Moreover, the limit of detection can fall into the maximum acceptable level of 1.3 ppm (~20 μM) set by USEPA.

Table 2 Various spectrofluorimetric and spectrophotometric sensing systems for determination of Cu^{2+}.

Method	System	Detection range (μM)	Ref.
Fluorescence	Amplex^R UltraRed / hydrogen peroxide	1.6-12	[26]
	Rhodamine spirolactam derivative	0.8-10	[27]
	Coumarin derivative	0.1-1.0	[28]
	p-Cresol / hydrogen peroxide	0.3-50	[29]
	Luminescent porous silicon nanoparticles	1.0-10	[30]
	Glutathione protected gold nanoclusters	0.1-6.25	[31]
	bis-Pyrene derivative	1.0-15	[32]
	N-(quinoline-8-yl)-2-(3-triethoxysilyl-propylamino) -acetamide grated silica nanoparticles	2.0-20	[33]
	Fe_3O_4 @ CdTe Core/Shell Microspheres	1.0-10	[34]
	Spiropyran functionalized semiconducting polymer dots	0.0-60	[35]
Absorption	Peptide / gold nanoparticles	10-150	This Study
	DNA / click chemistry	0.5-10	[36]
	DNAzyme / gold nanoparticles	0.625-15	[37]
	Starch-stabilized silver nanoparticles	0.1-10	[38]
	In situ formation of silver nanoparticles	0.25-2.0	[39]

3.5 Selectivity of the colorimetric Cu^{2+} sensor

The selectivity of Cu^{2+} sensor proposed in this work has also been examined under the interference of other cations, such as Mg^{2+}, Ca^{2+}, Zn^{2+}, Fe^{3+}, Pb^{2+}, Mn^{2+}, Ba^{2+}, Ni^{2+}, Co^{2+}, K^{+} and Ag^{+}. Figure 5 shows the histogram of the absorbance change $(Ao_{520}-A_{520})$ / Ao_{520}, where Ao_{520} is the absorbance at 520 nm without Cu^{2+} and A_{520} stands for the absorbance after incubation with the ions. At the same concentration of 100 μM, copper (II) ions can induce the most decrease of UV-vis absorbance at 520 nm. Nevertheless, except for Zn^{2+}, other ions like Ni^{2+}, Co^{2+}, Ba^{2+},Mn^{2+}, Fe^{3+}, Mg^{2+}, $Ca^{2+}$and K^{+} has no obvious effects on the sensing. Also, it is interesting that in the presence of Pb^{2+} or Ag^{+}, the UV-vis absorbance at 520 nm is enhanced slightly rather than reduced. Moreover, an elevated concentration of 1 mM ions was performed with similar results (data not shown).

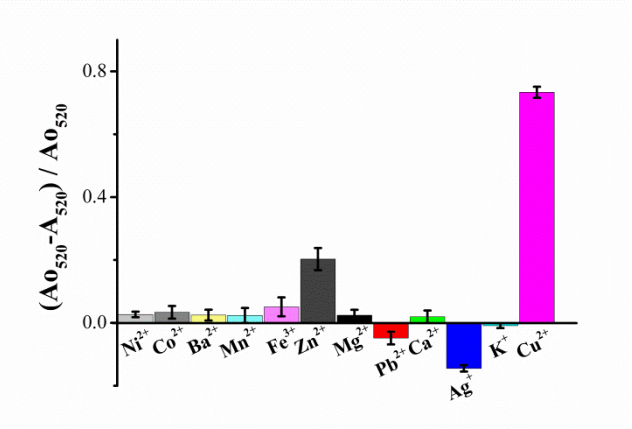

Fig. 5 Absorbance change histogram of various ions in the same concentration of 100 μM upon to copper (II) ions. Data was recorded in 10 mM HEPES (pH 8.0) at room temperature. The scale bars represent the standard deviations of three replicated samples.

4. Conclusion

In conclusion, a simple colorimetric sensor, which is based on the conformational change of Cu^{2+}-binding peptide and the induced simultaneous aggregation of AuNPs, has been developed for sensitive and selective determination of cooper (II) ions. Compared with previous methods based on the labeling of molecule beacons or organic synthesis of fluorescent compounds, this cost-effective approach shows excellent selectivity and sensitivity towards copper (II) ions. The detectable range is also broader than the previous reports and the limit of detection can fall into the maximum acceptable level of 1.3 ppm (~20 μM) set by USEPA. Therefore, it may have the potential application in monitoring drinking water and environmental contaminant. Furthermore, we expect that the present approach could be not only used in monitoring Cu^{2+} but also extended to other heavy metal ions by employing differential binding peptide.

Acknowledgements

This work is supported by the National Natural Science Foundation of China (Grant No. 61275085, 31100560).

[a]*Laboratory of Biosensing Technology, School of Life Sciences, Shanghai University, Shanghai 200444, P R China*
[b]*Department of Biochemistry and State Key Laboratory of Pharmaceutical Biotechnology, Nanjing University, Nanjing 210093, P R China. Fax: +86 25 83592510; E-mail address: genxili@nju.edu.cn.*

† Electronic Supplementary Information (ESI) available: UV-vis absorption spectra of BSA-absorbed gold nanoparticles before and after addition of copper (II) ions. See DOI: 10.1039/b000000x/

References

1. R. Elghanian, J. J. Storhoff, R. C. Mucic, R. L. Letsinger and C. A. Mirkin, *Science*, 1997, **277**, 1078-1081.
2. J. J. Storhoff, A. A. Lazarides, R. C. Mucic, C. A. Mirkin, R. L. Letsinger and G. C. Schatz, *J. Am. Chem. Soc.*, 2000, **122**, 4640-4650.
3. I. E. Sendroiu, S. F. Mertens and D. J. Schiffrin, *Phys. Chem. Chem. Phys.*, 2006, **8**, 1430-1436.
4. S. K. Ghosh and T. Pal, *Chem. Rev.*, 2007, **107**, 4797-4862.
5. T. E. Lin, W. H. Chen, Y. C. Shiang, C. C. Huang and H. T. Chang, *Biosens. Bioelectron.*, 2011, **29**, 204-209.
6. T. Gao, L. Ning, C. Li, H. Wang and G. Li, *Anal. Chim. Acta*, 2013, **788**, 171-176.
7. J. Zhao, T. Liu, Q. Fan and G. Li, *Chem. Commun.*, 2011, **47**, 5262-5264.
8. F. Xia, X. Zuo, R. Yang, Y. Xiao, D. Kang, A. Vallée-Bélisle, X. Gong, J. D. Yuen, B. B. Y. Hsu, A. J. Heeger and K. W. Plaxco, *P. Natl. Acad. Sci. USA*, 2010, **107**, 10837-10841.
9. Y. Jiang, H. Zhao, Y. Lin, N. Zhu, Y. Ma and L. Mao, *Angew. Chem.*, 2010, **122**, 4910-4914.
10. F. Li, J. Zhang, X. Cao, L. Wang, D. Li, S. Song, B. Ye and C. Fan, *Analyst*, 2009, **134**, 1355-1360.
11. F. Wang, X. Liu, C.-H. Lu and I. Willner, *ACS Nano*, 2013, **7**, 7278-7286.
12. J. Wang, L. Wang, X. Liu, Z. Liang, S. Song, W. Li, G. Li and C. Fan, *Adv. Mater.*, 2007, **19**, 3943-3946.
13. C.-Y. Lin, C.-J. Yu, Y.-H. Lin and W.-L. Tseng, *Anal. Chem.*, 2010, **82**, 6830-6837.
14. Z. Wang, J. H. Lee and Y. Lu, *Adv. Mater.*, 2008, **20**, 3263-3267.
15. X. Zhu, J. Zhao, Y. Wu, Z. Shen and G. Li, *Anal. Chem.*, 2011, **83**, 4085-4089.
16. X. Zhu, Y. Cao, Z. Liang and G. Li, *Protein Cell*, 2010, **1**, 842-846.
17. C. D. Medley, J. E. Smith, Z. Tang, Y. Wu, S. Bamrungsap and W. Tan, *Anal. Chem.*, 2008, **80**, 1067-1072.
18. X. Xu, M. S. Han and C. A. Mirkin, *Angew. Chem.*, 2007, **119**, 3538-3540.
19. W. Zhao, M. A. Brook and Y. Li, *Chembiochem*, 2008, **9**, 2363-2371.
20. E. L. Que, D. W. Domaille and C. J. Chang, *Chem. Rev.*, 2008, **108**, 1517-1549.
21. A. Prisecaru, M. Devereux, N. Barron, M. McCann, J. Colleran, A. Casey, V. McKee and A. Kellett, *Chem. Commun.*, 2012, **48**, 6906-6908.
22. A. P. Nugroho and H. Frank, *Toxico. Enviro. Chem.*, 2012, **94**, 918-929.
23. C. T. Sheline and D. W. Choi, *Ann. Neurol.*, 2004, **55**, 645-653.
24. C. E. Jones, S. R. Abdelraheim, D. R. Brown and J. H. Viles, *J. Biol. Chem.*, 2004, **279**, 32018-32027.
25. C. Hureau and P. Faller, *Biochimie*, 2009, **91**, 1212-1217.
26. C. Y. Tsai and Y. W. Lin, *Analyst*, 2013, **138**, 1232-1238.
27. Y. Zhao, X.-B. Zhang, Z.-X. Han, L. Qiao, C.-Y. Li, L.-X. Jian, G.-L. Shen and R.-Q. Yu, *Anal. Chem.*, 2009, **81**, 7022-7030.
28. K. Li, N. Li, X. Chen and A. Tong, *Anal. Chim. Acta*, 2012, **712**, 115-119.
29. H. Cao, W. Shi, J. Xie and Y. Huang, *Anal. Methods*, 2011, **3**, 2102.
30. B. Xia, W. Zhang, J. Shi and S. Xiao, *Analyst*, 2013, **138**, 3629-3632.

31. G. Zhang, Y. Li, J. Xu, C. Zhang, S. Shuang, C. Dong and M. M. F. Choi, *Sensor. Actuat. B Chem.*, 2013, **183**, 583-588.
32. L. Ding, S. Wang, Y. Liu, J. Cao and Y. Fang, *J. Mater. Chem. A*, 2013, **1**, 8866.
33. J. Zheng, C. Xiao, Q. Fei, M. Li, B. Wang, G. Feng, H. Yu, Y. Huan and Z. Song, *Nanotechnology*, 2010, **21**, 045501.
34. H. Wang, L. Sun, Y. Li, X. Fei, M. Sun, C. Zhang, Y. Li and Q. Yang, *Langmuir*, 2011, **27**, 11609-11615.
35. P. J. Wu, J. L. Chen, C. P. Chen and Y. H. Chan, *Chem. Commun.*, 2013, **49**, 898-900.
36. Q. Shen, W. Li, S. Tang, Y. Hu, Z. Nie, Y. Huang and S. Yao, *Biosens. Bioelectron.*, 2013, **41**, 663-668.
37. Y. Wang, F. Yang and X. Yang, *Nanotechnology*, 2010, **21**, 205502.
38. L.-J. Miao, J.-W. Xin, Z.-Y. Shen, Y.-J. Zhang, H.-Y. Wang and A.-G. Wu, *Sensor. Actuat. B Chem.*, 2013, **176**, 906-912.
39. X. Yuan and Y. Chen, *Analyst*, 2012, **137**, 4516-4523.
40. X. Wang, I. Bergenfeld, P. S. Arora and J. W. Canary, *Angew. Chem.*, 2012, **124**, 12265-12267.
41. J. Wang, W. Meng, X. Zheng, S. Liu and G. Li, *Biosens. Bioelectron.*, 2009, **24**, 1598-1602.
42. N. Li, Y. Xiang and A. Tong, *Chem. Commun.*, 2010, **46**, 3363-3365.
43. S. Sirilaksanapong, M. Sukwattanasinitt and P. Rashatasakhon, *Chem. Commun.*, 2012, **48**, 293-295.
44. J. Huang, Q. Zheng, J.-K. Kim and Z. Li, *Biosens. Bioelectron.*, 2013, **43**, 379-383.
45. L. Guo, Y. Xu, A. R. Ferhan, G. Chen and D. H. Kim, *J. Am. Chem. Soc.*, 2013, **135**, 12338-12345.
46. J. J. Storhoff, R. Elghanian, R. C. Mucic, C. A. Mirkin and R. L. Letsinger, *J. Am. Chem. Soc.*, 1998, **120**, 1959-1964.
47. K. H. Su, Q. H. Wei, X. Zhang, J. J. Mock, D. R. Smith and S. Schultz, *Nano Lett.*, 2003, **3**, 1087-1090.
48. P. K. Jain, W. Huang and M. A. El-Sayed, *Nano Lett.*, 2007, **7**, 2080-2088.

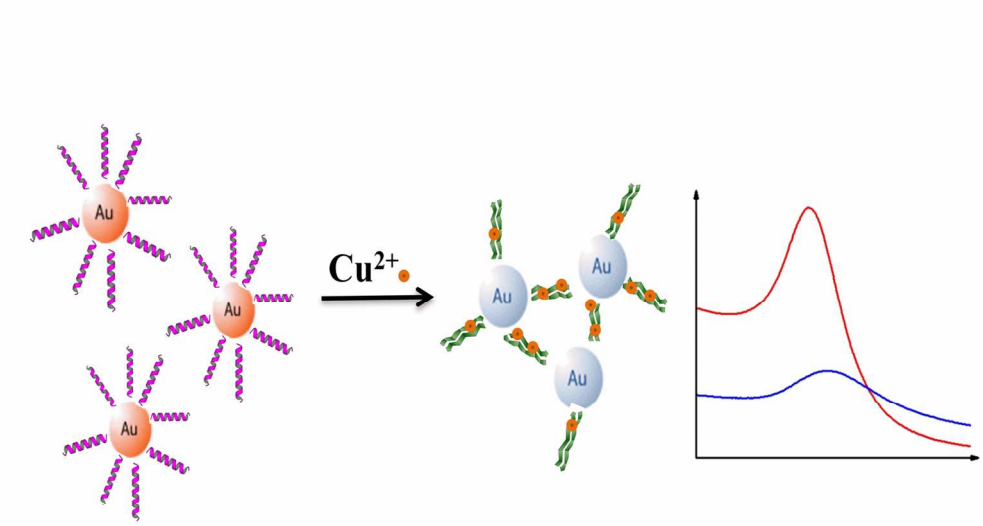

296x209mm (150 x 150 DPI)